J. Fluid Mech. (2010), *vol.* 646, *pp.* 517–526.
doi:10.1017/S0022112009993661

Reynolds-number dependency in homogeneous, stationary two-dimensional turbulence

ANNALISA BRACCO[1]† AND JAMES C. MCWILLIAMS[2]

[1]EAS and CNS, Georgia Institute of Technology, Atlanta, GA 30332, USA

[2]Department of Atmospheric and Oceanic Sciences and IGPP, UCLA, Los Angeles, CA 90095, USA

(Received 12 September 2009; revised 24 November 2009; accepted 24 November 2009)

Turbulent solutions of the two-dimensional Navier–Stokes equations are a paradigm for the chaotic space–time patterns and equilibrium distributions of turbulent geophysical and astrophysical 'thin' flows on large horizontal scales. Here we investigate how homogeneous, stationary two-dimensional turbulence varies with the Reynolds number (Re) in stationary solutions with large-scale, random forcing and viscous diffusion, also including hypoviscous diffusion to limit the inverse energy cascade. This survey is made over the computationally feasible range in $Re \gg 1$, approximately between 1.5×10^3 and 5.6×10^6. For increasing Re, we witness the emergence of vorticity fine structure within the filaments and vortex cores. The energy spectrum shape approaches the forward-enstrophy inertial-range form k^{-3} at large Re, and the velocity structure function is independent of Re. All other statistical measures investigated in this study exhibit power-law scaling with Re, including energy, enstrophy, dissipation rates and the vorticity structure function. The scaling exponents depend on the forcing properties through their influences on large-scale coherent structures, whose particular distributions are non-universal. A striking result is the Re independence of the intermittency measures of the flow, in contrast with the known behaviour for three-dimensional homogeneous turbulence of asymptotically increasing intermittency. This is a consequence of the control of the tails of the distribution functions by large-scale coherent vortices. Our analysis allows extrapolation towards the asymptotic limit of $Re \to \infty$, fundamental to geophysical and astrophysical regimes and their large-scale simulation models where turbulent transport and dissipation must be parameterized.

1. Introduction

Since Kolmogorov's work (1941, 1962), the prevailing paradigm for isotropic, homogeneous, stationary fluid turbulence at large Reynolds number (Re) has been the statistical dynamical independence of Re in the energy inertial range, i.e. on scales between energy injection and dissipation. Theoretical attempts to assess this premise for three-dimensional turbulent flows face a great computational challenge to reach large Re and the unresolved question of whether smooth initial conditions and forcing always yield non-singular, long-time solutions. Two-dimensional turbulence, on the other hand, is computationally more accessible, is non-singular (Ladyzhenskaya

† Email address for correspondence: abracco@gatech.edu

1969), and has deep connections to the behaviour of flows subject to rapid rotation and density stratification as the atmosphere and ocean (Charney 1971) and magnetic stratified fluids (Paret & Tabeling 1997). Theoretical studies with a statistical description assuming isotropy and homogeneity predict a dual cascade, with a forward cascade of enstrophy (vorticity variance) towards small scales and an inverse cascade of energy (Kraichnan 1967; Batchelor 1969). In the limit of infinite domain size and zero viscosity, the predicted isotropic energy wavenumber spectrum shape is $k^{-5/3}$ in the inverse cascade range, verified in both laboratory experiments (Paret & Tabeling 1997) and numerical simulations (Borue 1994; Boffetta, Celani & Vergassola 2000), and it is k^{-3} in the inverse range (with possible logarithmic corrections; Kraichnan 1971), with slightly steeper spectrum slopes generally reported in numerical simulations (Borue 1993; Gotoh 1998; Pasquero & Falkovich 2002). The departures from statistical–theoretical predictions in two-dimensional turbulence are usually associated with the spontaneous emergence of long-lived coherent vortices (McWilliams 1984; Bracco *et al.* 2000*b*). Theoretical studies also predict a universal behaviour of scaling exponents for steady two-dimensional turbulence in the direct cascade regime independent of the forcing, under the assumptions that coherent vortices are isolated entities that do not contribute to the small-scale correlation functions (Falkovich & Lebedev 1994; Eyink 1995).

The aim of this paper is to examine the central idea of classical turbulence that the equilibrium statistical properties of the flow are invariant as long as Re is sufficiently high, focusing on the enstrophy cascade range in stationary two-dimensional turbulence with random forcing at small k and damping at both large and small wavenumbers. Prototypes for this kind of calculation are described by Borue (1993) and Schorghofer (2000*a*).

2. Model formulation

The vorticity equation for a two-dimensional flow is

$$\frac{\mathrm{D}\omega}{\mathrm{D}t} = \frac{\partial\omega}{\partial t} + J[\psi, \omega] = D + F. \tag{2.1}$$

Here ω is the relative vorticity ($\omega = (\partial^2\psi/\partial x^2) + (\partial^2\psi/\partial y^2) = \Delta\psi$). Note that ψ is the streamfunction (related to velocity components by $u = -(\partial\psi/\partial y)$, $v = \partial\psi/\partial x$). Similarly, Δ is a two-dimensional Laplacian operator and J is a two-dimensional Jacobian operator ($J[\psi, \omega] = (\partial\psi/\partial x)(\partial\omega/\partial y) - (\partial\psi/\partial y)(\partial\omega/\partial x)$). Note also that $D = \mu\Delta^{-1}\omega + \nu\Delta\omega$ is a generalized damping term composed of a physically artificial hypoviscosity μ to provide an energy sink at small k to balance the inverse energy cascade and a conventional viscosity to provide an enstrophy sink at large k. We verified that the alternative use of Ekman drag ($\propto -\omega$) to dissipate energy at large scales provides analogous results albeit with a narrower inertial range in k. The forcing F acts only at large scales in an isotropic shell $[k_0 - \mathrm{d}k, k_0 + \mathrm{d}k]$ with $k_0 = 4$ and $\mathrm{d}k = 1$. It has a fixed spectrum amplitude a, but random phase ϕ in wavenumber vector $\boldsymbol{k}$ that ensures an incoming energy input rate

$$Q_E = -\int F\psi \, \mathrm{d}\boldsymbol{x}.$$

Thus, Q_E changes randomly with time but has a constant long-time average. Note that ϕ is determined by a Markov process with a memory time t_F. Because the energy input Q_E depends on the solution at the forcing wavenumber, we can compare energy

Case parameters			
Re	*N*	ν	$-\alpha$
($a = 0.14$,	$t_F = 0.005$,	$\mu = 1.5$)	
1.5×10^3	256	1.0×10^{-3}	-4.10 ± 0.15
1.0×10^4	512	3.0×10^{-4}	-3.80 ± 0.13
6.7×10^4	1024	8.5×10^{-5}	-3.45 ± 0.10
3.3×10^5	2048	2.5×10^{-5}	-3.27 ± 0.08
1.4×10^6	4096	1.2×10^{-5}	-3.19 ± 0.05
5.6×10^6	8192	4.6×10^{-6}	-3.10 ± 0.03
($a = 0.005$,	$t_F = \infty$,	$\mu = 1.65$)	
1.7×10^3	256	2.5×10^{-3}	-3.87 ± 0.15
6.4×10^3	512	8.5×10^{-4}	-3.62 ± 0.13
3.2×10^4	1024	2.5×10^{-4}	-3.41 ± 0.10
1.3×10^5	2048	9.0×10^{-5}	-3.30 ± 0.08

TABLE 1. Parameters used in this study for the set of runs with $t_F = 0.005$ and $t_F = \infty$. The right-end column is the negative power-law exponent of the energy spectrum calculated in the inertial range by a least-square fit. Errors are based on the spread between single-time fits. The spectra have been averaged over 13 different times for $N \geqslant 1024$ and over 26 frames for the three lowest N cases.

transfer rates for increasing *Re*. This forcing procedure differs from the temporally white random forcing used by Borue (1993), and it allows coherent vortices to form without immediate disruption by the forcing. Below we will focus on a set of runs with $t_F = 0.005$ chosen to be 1 order of magnitude shorter than the eddy turnover time at $Re \approx 7 \times 10^4$. We verified that the principal conclusions about *Re* dependency hold for a larger value of memory time, $t_F = 0.07$, with corresponding reduction of a. A third set of runs, spanning a more limited *Re* range, has been computed using fixed ϕ, equivalent to having $t_F = \infty$ and a much smaller amplitude of the forcing function, and is briefly discussed for comparison. All integrations are performed using a standard pseudo-spectral code with 2/3 de-aliasing and a third-order Adams–Bashforth time-integration scheme in a doubly periodic domain with size $L = 2\pi$. The viscosity ν at each grid-size $N \times N$ has been chosen to maximize the resulting *Re* while avoiding spurious oscillations (computational noise). The same F and μ are used in runs with different *Re*. A list of parameters is given in table 1.

The terms E and Z are spatially averaged mean energy and enstrophy, respectively, defined by

$$E = \frac{1}{2L^2} \int (\nabla \psi)^2 \, \mathrm{d}x \, \mathrm{d}y, \tag{2.2}$$

$$Z = \frac{1}{2L^2} \int (\nabla^2 \psi)^2 \, \mathrm{d}x \, \mathrm{d}y, \tag{2.3}$$

and they are reported here as time averaged. The Reynolds number is defined as $Re = U/\nu k_E$, where U is the root-mean-square (r.m.s.) velocity of the flow, $\sqrt{2E}$, and k_E is the centroid wavenumber, $k_E = (\int k E(k) \, \mathrm{d}k)/(\int E(k) \, \mathrm{d}k)$. Each integration is run for at least 5×10^4 eddy turnover times, $t_e = 1/\sqrt{Z}$, once stationarity is reached, to ensure accuracy in the flow statistics. In statistical equilibrium, the energy and

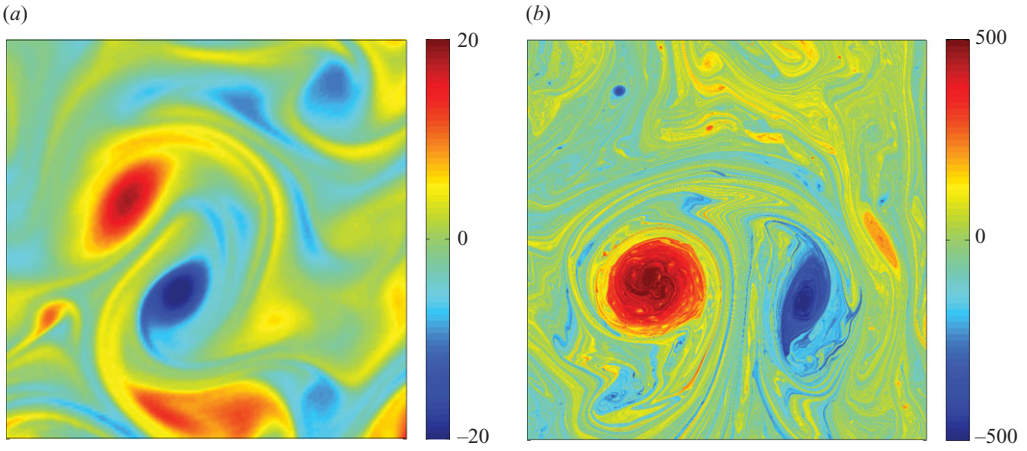

FIGURE 1. Instantaneous vorticity fields for $t_F = 0.005$ for (*a*) $Re \approx 1.5 \times 10^3$ ($N = 256$) and (*b*) $Re \approx 5.6 \times 10^6$ ($N = 8192$). In both (*a*, *b*), 1/4 of the whole $[2\pi \times 2\pi]$ domain is shown.

enstrophy balances for (2.1) are

$$\langle Q_E \rangle = \epsilon_\mu + \epsilon_\nu, \quad \langle Q_Z \rangle = \chi_\mu + \chi_\nu, \tag{2.4}$$

where $\langle \cdot \rangle$ is a space–time average, $Q_Z = \int F\omega \, \mathrm{d}\boldsymbol{x}$, and the small- and large-scale energy and enstrophy dissipation rates are, respectively,

$$\epsilon_\nu = \nu \langle \omega^2 \rangle, \quad \epsilon_\mu = \mu \langle \psi^2 \rangle, \tag{2.5}$$

$$\chi_\nu = \nu \langle | \nabla \omega |^2 \rangle, \quad \chi_\mu = \mu \langle | \nabla \psi |^2 \rangle. \tag{2.6}$$

Because our solutions have a forward enstrophy cascade to dissipation, we define a wavenumber that indicates the onset of the dissipation range (analogous to the inverse Kolomogorov scale in three-dimensions)

$$k_\nu = \left(\frac{\chi_\nu}{\nu^3} \right)^{1/6}. \tag{2.7}$$

3. Results

For all *Re*, the flow dynamics are dominated by the presence of coherent vortices. The number of large eddies at or just below the forcing scale k_0^{-1} does not vary significantly between the different resolutions for identical forcing. For $Re > 10^5$, very small vortices emerge in between the large eddies, and a fine structure emerges in the vorticity field within intense filaments and even in vortex cores (figure 1). For decreasing ν, the time for axisymmetrization of the large eddies increases, and intense vorticity filaments persist inside the large vortices in addition to the more familiar peripheral filaments (McWilliams 1984). With a finite t_F, the large coherent vortices at the forcing scale are extremely persistent, while in the set of simulations with smaller forcing amplitude and $t_F = \infty$, fewer and far shorter-living large vortices develop (figure 2) because of the very small spectral amplitude of the forcing.

The energy spectrum in the inertial range flattens towards the classical k^{-3} limit (Kraichnan 1967; Batchelor 1969) as *Re* increases (figure 3*a*) for all cases, in agreement with previous works (Borue 1993; Schorghofer 2000*a*; Boffetta 2007). A simple power law (table 1) describes the spectral functional form here better than the logarithmically

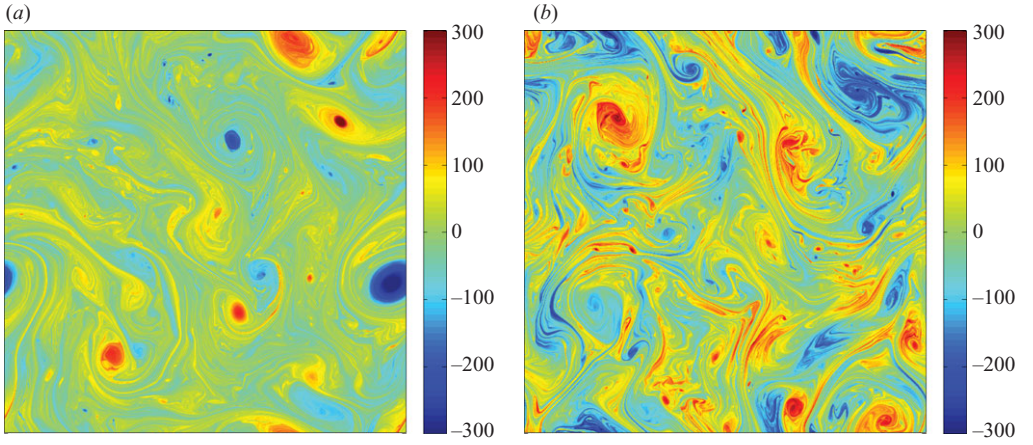

FIGURE 2. Instantaneous vorticity fields for (*a*) $t_F = 0.005$ and $Re \approx 3.3 \times 10^5$ ($N = 2048$) and (*b*) $t_F = \infty$ at $Re \approx 1.3 \times 10^5$ ($N = 2048$). The whole $[2\pi \times 2\pi]$ domain is shown.

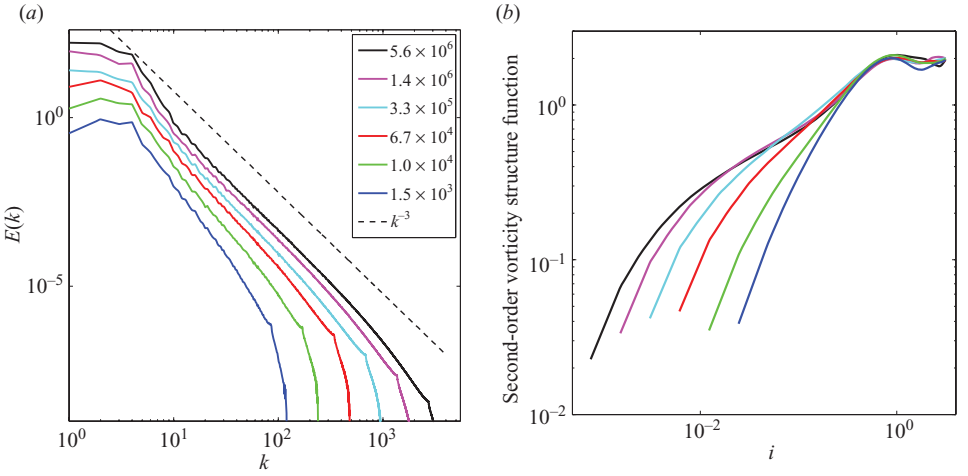

FIGURE 3. (*a*) Energy spectra and (*b*) second-order vorticity structure functions across the various Re for the set of experiments with finite forcing decorrelation time.

corrected one derived by Kraichnan (1971), which assumes that velocity gradients are δ-correlated in time. The logarithmic correction has been recovered only in numerical simulations of two-dimensional turbulent flows characterized by the absence of coherent vortices (Pasquero & Falkovich 2002). We also observe variations with Re in the efficiency of the energy cascade expressed by the local energy tendency, $\Sigma_E = \mathrm{d}v^2/\mathrm{d}t$. The probability density function (PDF) of Σ_E averaged over tens of snapshots to ensure convergence (not shown) reveals that both direct (positive Σ_E) and inverse (negative) tendencies are observed at all Re, indicating transfer of energy to both smaller and larger scales, but the inverse cascade becomes dominant for decreasing ν, as noted by Boffetta (2007). The shape of the PDF of enstrophy tendency, $\Sigma_Z = \mathrm{d}\omega^2/\mathrm{d}t$, on the other hand, does not vary with Re (not shown), but the inverse enstrophy cascade is particularly intense in vorticity filaments and around the core of the vortices, in agreement with the analysis of Babiano & Provenzale

(2007). Noticeably, we find that in all sets of runs the increase in E for increasing Re occurs at all k, notwithstanding identical μ and F. Such behaviour is reported by Schorghofer (2000*a*) limited to the intermediate scales in two-dimensional integrations with a similar forcing configuration but spanning a much shorter time interval. We find that a very long spin-up (several hundred eddy turnover times) is necessary to ensure statistically stationary spectra at low wavenumbers.

The changes in spectral slopes with Re are mirrored in the behaviour of the second-order vorticity structure functions

$$\langle \delta\omega(l)^2 \rangle = \langle |\omega(\boldsymbol{x}+\boldsymbol{l}) - \omega(\boldsymbol{x})|^2 \rangle, \tag{3.1}$$

with $l = |\boldsymbol{l}|$ being the spatial separation distance (figure 3*b*). In the context of passive scalar transport, Benzi, Paladin & Vulpiani (1990) have shown that for a given energy spectrum $E(k) \sim k^{\alpha} = k^{-3-d}$ with $d > 0$, in the limit of infinite Re and in the absence of large-scale dissipation, $\langle \delta\omega(l)^2 \rangle \sim l^d$. Although the rate at which both energy spectra and vorticity structure functions flatten for increasing Re is properly described by the relation above, we empirically find that the structure function slopes are slightly steeper than those predicted by Benzi *et al.* (1990) calculation. As demonstrated by Babiano & Provenzale (2007), the scale-to-scale transfers of enstrophy and passive scalar variance differ in the inertial range because of anomalous enstrophy transfers within the vortices and in the elliptic regions around them, and vorticity structure function slopes are indeed steeper than the passive scalar ones. The global regularity of the Navier–Stokes equations in two-dimensions implies that the second-order velocity structure function velocity is $\langle \delta v(l)^2 \rangle \sim l^2$ in the limit of infinite Re, which implies $E(k) \sim k^{-\alpha}$ with $\alpha \geqslant 3$ (Rose & Sulem 1978; Benzi *et al.* 1990). The velocity structure functions (not shown) appear to be independent of Re, reflecting the approximate invariance of the shape of the spectrum at large scales in spite of the Re variations in the spectrum amplitude and value of α, and they compare reasonably well with the theoretical prediction.

The statistics of two-dimensional turbulent flows are further investigated with PDFs for streamfunction, velocity, vorticity and vorticity gradient at different Re. All PDFs are obtained by averaging 26 (for $Re < 10^5$) or 13 (for $Re > 10^5$) snapshots separated in time by at least 200 t_e, and their arguments are normalized by the standard deviation σ for each field at each Re. Independent of the field analysed, the distributions for each choice of t_F are invariant with respect to Re within sampling errors (Figure 4*a*,*b*). Vorticity and velocity distributions are non-Gaussian due to the presence of the vortices and the far-field velocity associated with them (McWilliams 1990; Bracco *et al.* 2000*a*), respectively, consistent with coherent vortex dominance in the tails of the PDFs. PDF tails reflect the nature of intermittency in the flow. The invariance of the PDFs is further shown by the absence of Re dependency in the velocity and vorticity kurtosis Ku (figure 4*c*; $Ku[\omega] \approx 7.1$ and $Ku[v] \approx 4.5$ for $t_F = 0.005$; not shown $Ku[\omega] \approx 3.8$ and $Ku[v] \approx 3.2$ for $t_F = \infty$, while intermediate values are found for $t_F = 0.07$ and when Ekman drag is used). This result extends the analysis of Schorghofer (2000*b*), where similar but not at all identical shapes for the PDFs were found for different Re and is fundamental to the extrapolation towards the limit $Re \to \infty$ in the presence of coherent vortices. We verified for all our sets of runs that, whenever the large-scale flow has reached a statistically stationary state, PDFs are indeed invariant in shape.

Even though the normalized PDFs do not vary with the Reynolds number, the field magnitudes do increase with Re (figure 5). We find that the dependencies have power-law forms, for example $E \sim Re^{\lambda_E}$ for $\lambda_E \approx 0.6 \pm 0.05$ in the set with $t_F = 0.005$.

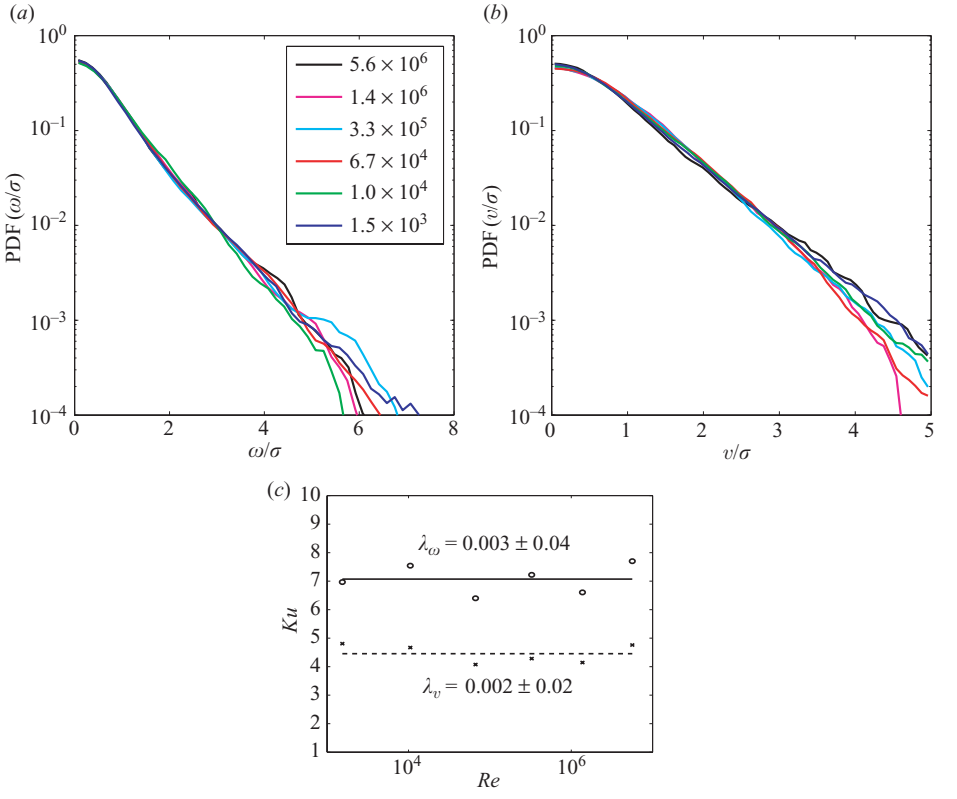

FIGURE 4. PDFs of (*a*) vorticity and (*b*) velocity at the various *Re* or the set of experiments with finite forcing decorrelation time. (*c*) The kurtosis of the distributions across *Re* for the vorticity (solid line) and the velocity distributions (dashed line), respectively.

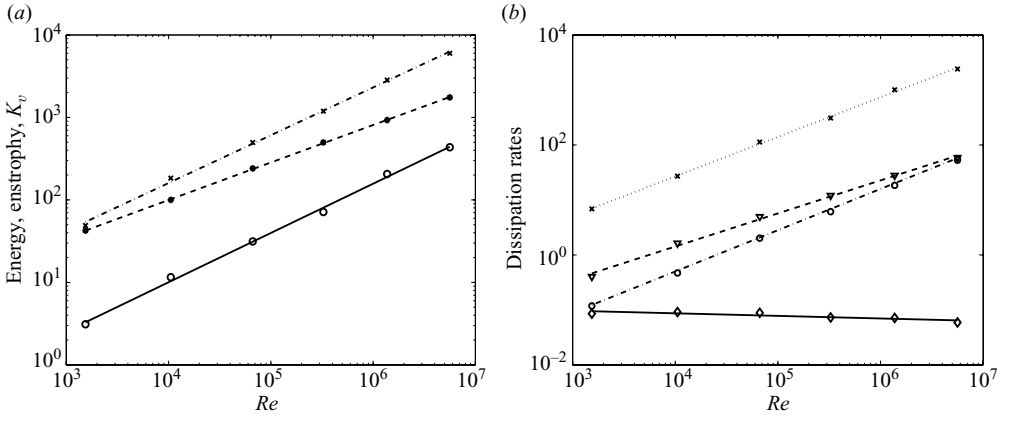

FIGURE 5. *Re* scaling for (*a*) energy (solid), enstrophy (dash-dotted) and the equivalent Kolmogorov scale, K_v (dashed) and (*b*) energy and enstrophy dissipation rates: ϵ_v (solid), χ_v (dash-dotted), ϵ_μ (dotted), χ_μ (dashed).

Table 2 lists λ values for other variables based on a least-square logarithmic fit and the associated estimation error in the slope for two of our sets of runs. Person's chi-square tests confirm the statistical significance. Power-law dependencies are found for all the

Power-law exponents		
Variable	$\lambda, t_f = 0.005$	$\lambda, t_f = \infty$
k_E	-0.042 ± 0.001	-0.045 ± 0.002
k_ν	0.455 ± 0.002	0.46 ± 0.02
E	0.60 ± 0.05	0.36 ± 0.02
Z	0.58 ± 0.04	0.37 ± 0.01
$(\nabla\omega)^2$	1.41 ± 0.05	1.26 ± 0.03
ϵ_ν	-0.05 ± 0.06	-0.38 ± 0.03
ϵ_μ, ψ^2	0.72 ± 0.05	0.48 ± 0.02
χ_ν	0.75 ± 0.05	0.49 ± 0.04
χ_μ	0.60 ± 0.10	0.37 ± 0.01

TABLE 2. List of exponents λ for the power-law scaling of the Re dependencies for various quantities for $t_F = 0.005$ and $t_F = \infty$.

solution sets we have obtained using different values for k_0, μ (or an Ekman drag counterpart) and t_F. The fitted exponent values, however, are not universal, although they do have the same signs and similar relationships among the different variables; the exponents depend on the forcing function through its influence on the large-scale coherent structures. Because of the non-universality, we have not attempted to make a theory for the λ values. In our method of posing the calculations, we choose decreasing ν with increasing resolution N, hence increasing Re. The *post facto* Re dependencies are $\lambda_\nu = -0.66$ and $\lambda_N = 0.42$ for $t_F = 0.005$, and $\lambda_\nu = -0.76$ and $\lambda_N = 0.47$ for $t_F = \infty$. A consistency check on our choices is that k_ν in (2.7) has essentially the same λ value as N, indicating that we have approximately kept the proportional resolution of the dissipation range constant in our solution set.

Note that E and Z have the same exponents within a given t_F solution set ($\lambda \sim 0.6$ and ~ 0.4 for $t_F = 0.005$ and $t_F = \infty$, respectively), which demonstrates similar scaling behaviours for the dominant part of the fields around the forcing and coherent vortex scales. The palenstrophy $\langle(\nabla\omega)^2\rangle$ increases much faster ($\lambda = 1.4$ and 1.3), showing the relative growth of small-scale variance with Re. The dominant dissipation rates are large-scale ϵ_μ for E and small-scale χ_ν for Z, consistent with the inverse-energy and forward-enstrophy cascades, respectively. Furthermore, they both have essentially the same exponent ($\lambda > 0.7$ and $\lambda \sim 0.5$ for $t_F = 0.005$ and $t_F = \infty$, respectively), as they should if Q_E and Q_Z have identical scaling with spectrally narrow-band forcing. This dissipation exponent is modestly larger than the exponent for E and Z, indicating that the throughputs are increasing somewhat faster than the contents due to increasing flow correlations with F in Q_E and Q_Z. Because $\langle\psi^2\rangle \propto \epsilon_\mu$, the throughput must increase somewhat faster than E and Z as the energy centroid k_E weakly shrinks ($\lambda \simeq -0.04$ for all forcing considered) and moves deeper into the hypoviscous dissipation range. The secondary dissipation rates have weaker Re dependencies for finite t_F (i.e. $\lambda \approx 0$ for small-scale ϵ_ν, and $\lambda = 0.6$ for large-scale χ_μ), to be compared to $\lambda \approx -0.4$ for ϵ_ν and $\lambda \approx 0.4$ for χ_μ when $t_F = \infty$; those exponents imply that the inverse and forward cascades become increasingly distinct at large Re. The normalized rate of small-scale energy dissipation, $r_E = \epsilon_\nu / E \sim Re^{-0.65}$ and $\sim Re^{-0.74}$ for finite and infinite t_F, respectively, is vanishingly small, even as the eddy turnover rate, $t_e^{-1} \sim Re^{0.3}$ and $\sim Re^{0.4}$, increases with stronger flow. In our solutions with $t_F = 0.005$, ϵ_ν vanishes much slower than in one of our alternative sets with $t_F = \infty$, where the vortex component is visibly less dominant, and we find $\epsilon_\nu \sim Re^{-0.4}$.

Alexakis & Doering (2006) derived a theoretical prediction of ϵ_ν for a broad class of imposed large-scale forcing but under the classical assumptions about homogeneity, isotropy and k-local nonlinear interaction, hence neglecting the role of the coherent vortices, and fixed velocity and centroid wavenumber. In their results, the Re scaling for ϵ_ν is bounded by $\leqslant k_E U^3 Re^{-1/2}$. In all our solution sets with different forcings, all of ϵ_ν, $U \sim E^{1/2}$, and k_E vary with Re, but the normalized dissipation rate has essentially identical scaling, independent of the forcing, and for the range of Reynolds numbers considered, it lies well within their estimate:

$$\frac{\epsilon_\nu}{k_E U^3} \simeq Re^{-0.9} < Re^{-1/2}. \tag{3.2}$$

4. Discussion and conclusions

In summary, we analysed numerical solutions for randomly forced, stationary, homogeneous two-dimensional turbulence to examine their dependencies on Reynolds number (Re). The principal conclusions are as follows:

(i) Coherent vortices dominate the flow near the forcing scale and further emerge at small scales, also within the filaments and vortex cores, when Re is large enough;

(ii) The energy spectrum and second-order structure functions show simple, previously anticipated scaling behaviours;

(iii) The intermittency of the flows expressed in distribution functions is asymptotically invariant with Re. This is in contrast to the known growing intermittency in three-dimensional turbulence (e.g. $Ku[\omega] \sim Re^{1/3}$; Sreenivasan & Antonia 1997); and

(iv) Energy, enstrophy and their dissipation rates show simple power-law Re dependencies with increasing relative dominance by large-scale energy dissipation and small-scale enstrophy dissipation.

The last two conclusions are novel and provide for the first time a test of universality theories for two-dimensional turbulent flows taking into account the far field and the spatial velocity correlations associated with the coherent vortices. Indeed, with this work we have shown that even at large Reynolds numbers (up to at least $\sim 10^7$) power-law exponents and the value of the intermittency measures are non-universal; thus, a fundamental theory cannot be developed. We associate non-universality of scaling exponents with the variety of coherent vortex populations arising with different random forcing properties, especially t_F, and probably the large-scale damping mechanism (only slightly explored here). Nevertheless, the general character of Re scaling is similar across the different solution sets we examined, in particular the asymptotic invariance of the intermittency measures. These results allow extrapolation towards the asymptotic limit of $Re \to \infty$, relevant to geophysical and astrophysical regimes and their large-scale simulation models where turbulent transport and dissipation must, at least partly, be parameterized.

Support and computer time from the ARSC in Fairbanks have been invaluable. We thank Martin P. King for helping with the parallelization of the turbulence code.

REFERENCES

Alexakis, A. & Doering, C. R. 2006 Energy and enstrophy dissipation in steady state two-dimensional turbulence. *Phys. Lett.* A **359**, 652–657.

Babiano, A. & Provenzale, A. 2007 Coherent vortices and tracer cascades in two-dimensional turbulence. *J. Fluid Mech.* **574**, 429–448.

Batchelor, G. K. 1969 Computation of energy spectrum in homogeneous two-dimensional turbulence. *Phys. Fluids Suppl.* **12**, 233–239.

Benzi, R., Paladin, G. & Vulpiani, A. 1990 Power spectra in two-dimensional turbulence. *Phys. Rev.* A **42**, 3654–3656.

Boffetta, G. 2007 Energy and enstrophy fluxes in the double cascade of two-dimensional turbulence. *J. Fluid Mech.* **589**, 253–260.

Boffetta, G., Celani, A. & Vergassola, M. 2000 Inverse energy cascade in two-dimensional turbulence: deviations from Gaussian behaviour. *Phys. Rev.* E **61**, R29–R32.

Borue, V. 1993 Spectral exponents of enstrophy cascade in stationary two-dimensional homogeneous turbulence. *Phys. Rev. Lett.* **71**, 3967–3970.

Borue, V. 1994 Inverse energy cascade in stationary two-dimensional homogeneous turbulence. *Phys. Rev. Lett.* **72**, 1475–1478.

Bracco, A., LaCasce, J. H., Pasquero, C. & Provenzale, A. 2000*a* The velocity distribution of barotropic turbulence. *Phys. Fluids* **12** (10), 2478–2488.

Bracco, A., McWilliams, J. C., Murante, G., Provenzale, A. & Weiss, J. B. 2000*b* Revisiting freely decaying two-dimensional turbulence at millennial resolution. *Phys. Fluids* **12** (11), 2931–2941.

Charney, J. 1971 Geostrophic turbulence. *J. Atmos. Sci.* **28**, 1087–1095.

Eyink, Gregory L. 1995 Exact results on scaling exponents in the two-dimensional enstrophy cascade. *Phys. Rev. Lett.* **74** (19), 3800–3803.

Falkovich, G. & Lebedev, V. 1994 Universal direct cascade in two-dimensional turbulence. *Phys. Rev.* E **50**, 3883–3899.

Gotoh, T. 1998 Energy spectrum in the inertial and dissipation ranges of two-dimensional steady turbulence. *Phys. Rev.* E **57**, 2984–2992.

Kolmogorov, A. N. 1941 Local structure of turbulence in an incompressible fluid for very large Reynolds number. *Dokl. Akad. Nauk. SSSR* **30**, 19–21.

Kolmogorov, A. N. 1962 A refinement of previous hypotheses concerning the local structure of turbulence in a viscous incompressible fluid at high Reynolds number. *J. Fluid Mech.* **13**, 82–85.

Kraichnan, R. H. 1967 Inertial ranges in two-dimensional turbulence. *Phys. Fluids* **10**, 1417–1423.

Kraichnan, R. H. 1971 Inertial range transfer in two- and three-dimensional turbulence. *J. Fluid Mech.* **47**, 525–535.

Ladyzhenskaya, O. 1969 *The Mathematical Theory of Viscous Incompressible Flow*. Gordon and Breach.

McWilliams, J. C. 1984 The emergence of isolated coherent vortices in turbulent flow. *J. Fluid Mech.* **146**, 21–43.

McWilliams, J. C. 1990 The vortices of two-dimensional turbulence. *J. Fluid Mech.* **219**, 361–385.

Paret, J. & Tabeling, P. 1997 Experimental observation of the two-dimensional inverse energy cascade. *Phys. Rev. Lett.* **79**, 2486–2489.

Pasquero, C. & Falkovich, G. 2002 Stationary spectrum of vorticity cascade in two-dimensional turbulence. *Phys. Rev.* E **65**, 056305.

Rose, H. A. & Sulem, P.-L. 1978 Fully developed turbulence and statistical mechanics. *J. Phys. France* **39**, 441–484.

Schorghofer, N. 2000*a* Energy spectra of steady two-dimensional turbulent flows. *Phys. Rev.* E **61** (6), 6572–6577.

Schorghofer, N. 2000*b* Universality of probability distributions among two-dimensional turbulent flows. *Phys. Rev.* E **61** (6), 6568–6571.

Sreenivasan, K. & Antonia, R. 1997 The phenomenology of small-scale turbulence. *Annu. Rev. Fluid Mech.* **29**, 435–472.